American Journal of Pathology, Vol. 161, No. 2, August 2002

The Mevalonate Pathway during Acute Tubular Injury

Selected Determinants and Consequences

Richard A. Zager,* Vallabh O. Shah,† Hemangini V. Shah,† Philip G. Zager,† Ali C. M. Johnson,* and Sherry Hanson*

From the Departments of Medicine, the University of Washington, and the Fred Hutchinson Cancer Research Center, Seattle, Washington; and the University of New Mexico Health Sciences Center,† Albuquerque, New Mexico*

Renal injury evokes tubular cholesterol accumulation, mediated in part by increased HMG CoA reductase (HMGCR) levels. The present study was undertaken to define potential molecular determinants of these changes and to ascertain the relative importance of increased cholesterol production *versus* mevalonate pathway-driven protein prenylation, on the emergence of the so-called postrenal injury "cytoresistant state." Cultured proximal tubule (HK-2) cells were subjected to Fe or ATP depletion injury, followed 1 to 24 hours later by assessments of: 1) sterol transcription factor expression (SREBP)-1 and -2); 2) HMGCR mRNA levels; and 3) Ras/Rho prenylation. HMGCR mRNA and Ras/Rho prenylation were also assessed after *in vivo* ischemic and Fe-mediated renal damage. Using specific inhibitors, the relative importance of protein prenylation *versus* terminal cholesterol synthesis on HK-2 cell susceptibility to injury was also assessed. Acute injury induced HK-2 cell SREBP disruption and reductions in HMGCR mRNA. Renal cortical HMGCR mRNA also fell in response to either *in vivo* ischemic or Fe-mediated oxidant damage. At 24 hours after *in vitro*/*in vivo* injury, a time of cholesterol buildup, no increase in Ras/Rho prenylation was observed. Prenylation inhibitors did not sensitize HK-2 cells to injury. Conversely, squalene synthase (terminal cholesterol synthesis) blockade sensitized HK-2 cells to both Fe and ATP depletion attack. We concluded that: 1) acute tubular cell injury can destroy SREBPs and lower HMGCR mRNA. This suggests that posttranscriptional/translational events are responsible for HMGCR enzyme and cholesterol accumulation after renal damage. 2) Injury-induced cholesterol accumulation appears dissociated from increased protein prenylation. 3) Cholesterol accumulation, per se, seems to be the dominant mechanism by which the mevalonate pathway contributes to the postrenal injury cytoresistant state. *(Am J Pathol 2002, 161:681–692)*

Previous work from this laboratory has demonstrated that within 18 to 24 hours of acute ischemic, toxic, obstructive, or immunological injury, renal cortical cholesterol accumulation results.[1–5] Given that each of these insults induces marked histological injury, it is tempting to postulate that this cholesterol accumulation is an adaptive response to overt tissue damage. However, subsequent observations from this laboratory indicate that acute physiological perturbations, such as heat shock, endotoxemia, or mild dehydration, can also increase renal cholesterol levels despite normal renal histology.[6] These findings have led us to conclude that renal cholesterol accumulation is part of a multifaceted renal stress response.[6] Indeed, that cholesterol increments can be observed even in the absence of increased heat shock protein expression points to the sensitivity, and ubiquitous nature, of this reaction.[6]

To date, this laboratory has partially characterized this cholesterol overload state as follows: 1) after renal stress, a lag time of ~18 to 24 hours is required for cholesterol accumulation to result.[1,2] 2) Increased renal tubular cell cholesterol synthesis is at least partially responsible for the cholesterol increments, based on observations that statin therapy can block this reaction in stressed cultured proximal tubular HK-2 cells.[2] 3) Increases in HMG CoA reductase (HMGCR) likely contribute to this response, given that its expression, as assessed by Western blot, is heightened after *in vivo* heat shock, renal ischemia, and glycerol-induced rhabdomyolysis.[5] 4) As free cholesterol rises, part of it becomes esterified, leading to massive increases (~50–100×) in tissue cholesteryl ester pools.[2–6] 5) The cholesterol accumulation causes an upregulation of caveolins,[6] a family of cholesterol-binding proteins that regulate caveolae microdomain function and formation within plasma membranes. 6) The degree of cholesterol accumulation closely mirrors the severity, and course, of the evolving renal damage.[4] and 7) Although all of the pathophysiological consequences of postrenal injury cholesterol accumulation have not been defined, a large body of experimental data[1,7,8] indicate

Supported by research grants from the National Institutes of Health (RO1-DK-54200, RO1-DK-38432, RO1-DK49347) and from Dialysis Clinics, Inc., Nashville, TN.

Accepted for publication May 13, 2002.

Address reprint requests to Richard A. Zager, M.D., Fred Hutchinson Cancer Research Center, 1100 Fairview Ave. N, Room D2-190, Seattle, WA 98109-1024. E-mail: dzager@fhcrc.org.

that it helps mediate the so-called "cytoresistant state" (ie, postinjury-associated reductions in proximal tubular cell susceptibility to additional forms of attack). The *in vivo* correlate of this cellular phenomenon is acquired resistance to acute renal failure (ARF).[9–14]

Given the seemingly ubiquitous nature of stress-induced cholesterol accumulation, the present study was undertaken to gain additional insights into the molecular mechanisms leading to its expression, and to gain additional support to mechanistically link it to the cytoresistant state. The following specific issues have been addressed: first, given that HMGCR is the rate-limiting step in cholesterol synthesis,[14,15] might increased enzyme expression in postinjured tissues stem from a genomic response, culminating in increased HMGCR mRNA, and hence, HMGCR protein, levels? Second, because SREBPs (sterol regulatory element-binding proteins) are the transcription factors that primarily regulate cholesterol homeostasis,[16–21] are these proteins acutely activated by cell injury, a process that requires their proteolysis? Third, although there is compelling evidence that tissue cholesterol content is a critical determinant of cellular susceptibility to injury, it is noteworthy that activation of the HMGCR/mevalonate pathway can potentially increase prenylation of a number of signaling molecules (eg, involving GTP-binding proteins such as Ras and Rho).[22,23] Because the latter can also modulate cell injury responses,[24–28] does postinjury mevalonate pathway activation/HMGCR enzyme accumulation impact the cytoresistant state via an increase in protein prenylation, and not simply by an increase in tissue cholesterol content? Experiments into each of these issues form the basis of this report.

Materials and Methods

In Vivo *Animal Models of Renal Injury: Glycerol and Postischemic ARF*

Glycerol-induced rhabdomyolysis and postischemic renal injury were chosen as the two ARF models for studying the above delineated issues. This is because each has previously been demonstrated to manifest all of the characteristic features of the acquired cytoresistance state (ie, resistance to ARF,[12,29] increases in cholesterol and HMGCR enzyme expression within renal cortex/proximal tubules[1,4,5]). Male CD-1 mice (25 to 35 g; Charles River Laboratories; Wilmington, MA), housed under standard vivarium conditions with free food and water access, were used.

Glycerol-Induced ARF

Mice were anesthetized with isoflurane for approximately 30 seconds and then injected with 8.5 ml/kg of 50% glycerol in equally divided doses into each upper hind limb. At selected times thereafter (2, 4, 24 hours), they were reanesthetized with pentobarbital (1 to 2 mg i.p.), and the kidneys were removed through a midline abdominal incision. For animals studied 24 hours after glycerol injection, blood samples were obtained from the inferior vena cava for blood urea nitrogen (BUN) analysis just before kidney resection. Simultaneously treated sham mice provided control samples. The kidneys were used for either HMGCR mRNA or Western blot (Ras/Rho) analysis, as described below.

Postischemic ARF

Mice were anesthetized with pentobarbital and then both renal pedicles were isolated through a midline abdominal incision and occluded for either 10 or 30 minutes with smooth vascular clamps, as previously described.[1] Body temperature was maintained at 36°C to 37°C during this period. After completion of the ischemic period, the clamps were removed, the abdominal incision sutured, and the mice were allowed to recover from anesthesia. After completing either a 1-hour or 24-hour reflow period, the mice were reanesthetized, a blood sample was obtained from the inferior vena cava for BUN determination (24-hour reflow experiments), and then the kidneys were resected. Cortical tissues from these mice, and from sham-operated mice, were collected and saved for either Ras/Rho Western blotting or for HMGCR mRNA analysis, as described below.

Specific in Vivo *Experiments*

HMGCR mRNA Levels after Glycerol-Induced Renal Injury

Eighteen mice were injected with glycerol, as noted above. At either 2, 4, or 24 hours after glycerol injection ($n = 6$ at each time point), the kidneys were removed and the cortices dissected. Simultaneously obtained cortical samples from 12 nonglycerol-treated mice were obtained to provide normal tissue samples. RNA was extracted and the samples were analyzed for HMGCR mRNA, as described below.

HMGCR mRNA after Fe-Induced Renal Injury

Although the glycerol model of ARF is mediated, in large part, by heme iron cytotoxicity, many other factors are also involved (muscle injury, hemolysis, cardiac/hepatic dysfunction, cytokine/tumor necrosis factor-α release).[30] Hence, potential changes in renal cortical HMGCR mRNA after glycerol injection cannot necessarily be attributed specifically to iron-mediated injury. Hence, a second model of *in vivo* Fe injury was used (ferric Fe injection; in the form of the Venofer, a clinically used Fe preparation used for Fe replacement in end-stage renal disease patients). Previous work from this laboratory has demonstrated that Venofer Fe is directly cytotoxic to tubular and endothelial cells, in part by inducing marked lipid peroxidation and cellular ATP depletion.[31] Five mice received an intramuscular injury of 100 μl of Venofer (2 mg of elemental ferric iron; American Reagent Laboratories, Shirley, NY). Three hours later, these mice and five control mice were deeply anesthetized and both kidney

and liver samples were resected (much of injected Venofer Fe is removed by the hepatic reticuloendothelial system). The tissues were then processed for HMGCR mRNA.

HMGCR mRNA Levels after Postischemic Renal Injury

Ten-Minute Ischemia Protocol: Eight mice were subjected to the 10-minute ischemia protocol, with half undergoing either the 1-hour or 24-hour reperfusion period. At the end of this time, the kidneys were removed and RNA was isolated for subsequent HMGCR mRNA analysis. Eight sham-operated mice provided control tissues.

Thirty-Minute Ischemia Protocol: To assess the impact of a more severe form of injury on renal cortical HMGCR mRNA, eight mice were subjected to a 30-minute bilateral renal ischemia protocol. Eight sham-operated mice served as controls. After completing a 24-hour reperfusion/sham reperfusion period, the mice were reanesthetized, a blood sample was obtained BUN, and then the kidney tissues were harvested for mRNA.

Hepatic HMGCR mRNA after Statin Treatment

As a positive control for the HMGCR mRNA analysis, three mice were fed a diet containing 10 mg of atorvastatin (Pfizer, Ann Arbor, MI) per gram of food, as previously described.[5] After 3 days on this diet, these mice and three pair-fed control mice were anesthetized and the livers were resected. The samples were subjected to RNA extraction, followed by polymerase chain reaction (PCR) analysis of HMGCR mRNA (see below). (Note: statin therapy, by inhibiting hepatic cholesterol synthesis, should cause a compensatory increase in hepatic HMGCR mRNA. Hence, an increase in the latter would serve as a positive biological control for HMGCR mRNA analysis.)

In Vivo *Assessment of Protein Prenylation in the Cytoresistant State*

Glycerol-Induced ARF: The following experiment was undertaken to ascertain whether the postrenal injury cholesterol overload state is accompanied by an increase in mevalonate pathway-mediated protein prenylation. Ras and Rho, two GTP-binding proteins that undergo prenylation modification,[22,23] were selected for these assessments. Four mice were subjected to glycerol treatment as noted below, followed 24 hours later by kidney extraction. The renal cortices were dissected and stored at −70°C until Western blot analysis for Ras and Rho (described below). Cortical tissues from four normal mice served as controls.

Postischemic ARF: Four mice were subjected to the 30-minute ischemia/24-hour reperfusion protocol, as noted above. The mice were reanesthetized, a blood sample was obtained from the inferior vena cava for BUN analysis, and then both kidneys were resected. Cortical tissues from these mice, and from four sham-operated mice, were collected and saved for Western blot Ras/Rho analysis (see below).

Cultured Proximal Tubular (HK-2) Cell Experiments

Assessment of HMGCR mRNA Levels after Fe and ATP Depletion Injury

Fe-Induced Injury: HK-2 cells, an immortalized human proximal tubular cell line,[32] were used for the following experiments. The cells were cultured in T-75 flasks with keratinocyte serum-free medium (K-SFM) as previously described.[32] After achieving near confluence, 16 flasks were divided into four experimental groups: 1) continued control incubation for 4 hours; 2) continued control incubation for 24 hours; 3) incubation with a Fe-induced oxidant challenge for 4 hours (10 μmol/L of ferrous ammonium sulfate complexed with equimolar hydroxyquinoline, a Fe siderophore that allows for intracellular Fe access; FeHQ[1]); and 4) incubation with 7.5 μmol/L of FeHQ for 24 hours. After completing these incubations, the flasks were iced and the cells were detached with a cell scraper. They were then pelleted and RNA was extracted for HMGCR mRNA analysis (see below).

ATP Depletion/Ca Overload Injury: Eight flasks of HK-2 cells were established as noted above and divided into two groups: 1) ATP depletion/Ca ionophore-induced injury [7.5 μmol/L antimycin A, 20 mmol/L 2-deoxyglucose, 10 μmol/L Ca ionophore A23187 (ADC), in 0.2% dimethyl sulfoxide; 0.1% ethanol[33]], or 2) incubation under continued control incubation conditions (with ADC vehicle). After 4 hours under these conditions, corresponding with severe ATP depletion,[33]) the cells were collected and RNA was extracted for subsequent HMGCR mRNA analysis, as described below.

Assessment of SREBP-1 and SREBP-2 Expression after Tubular Cell Injury

These experiments were undertaken to assess the impact of acute cell injury on SREBP-1 and -2 transcription factor expression. (Note: Only *in vitro*, not *in vivo*, experiments were conducted because of a lack of appropriate antibodies for probing murine SREBPs.)

Fe-Mediated Oxidative Injury: HK-2 cells were grown in 24 T-75 flasks. On achieving near confluence, they were divided into six equal groups as follows: groups 1 to 3, continued control incubation for 1, 4, or 24 hours; groups 4 and 5, incubation with 10 μmol/L FeHQ for 1 or 4 hours; and group 6, incubation with 7.5 μmol/L FeHQ for 24 hours. The cells were detached with a cell scraper, collected, and protein extracts were prepared. These were then stored at −70°C until SREBP-1 and -2 Western blot analysis, as described below.

ADC Injury: HK-2 cells, grown in 16 T-75 flasks, were divided into four equal groups as follows: 1) control incubation for 1 hour, 2) control incubation for 4 hours, 3) incubation with the above ADC challenge for 1 hour; and 4) the ADC challenge for 4 hours. The cells were then

harvested and the proteins extracted for Western blot analysis.

Mevastatin Treatment: The following experiment served as a positive control for detecting SREBP up-regulation. Six T-75 flasks were divided into two equal groups and incubated either with 10 μmol/L mevastatin (Sigma, St. Louis, MO) to inhibit HMGCR or mevastatin vehicle (0.1% ethanol). Twenty-four hours later, the cells were detached and the proteins extracted for SREBP-1 and -2 Western blot analysis.

Assessment of HK-2 Cell Ras and Rho Prenylation

HK-2 cells were cultured in nine T-75 flasks, as noted above. On reaching near confluence, the flasks were divided into three equal groups: 1) continued control incubation, 2) incubation with 7.5 μmol/L FeHQ, and 3) incubation with 10 μmol/L mevastatin. (The purpose of the mevastatin group was to serve as a positive control, because HMGCR inhibition should decrease protein prenylation.) After completing 24-hour incubations, cell protein extracts were prepared and probed for Ras and Rho by Western blotting.

Impact of Protein Prenylation Inhibitors on HK-2 Cell Susceptibility to Injury

The following experiments were undertaken to ascertain the impact of protein prenylation on cellular susceptibility to injury. HK-2 cells were maintained under routine culture conditions in T-75 flasks with K-SFM, as noted above. At near confluence, the cells in each flask were detached by trypsinization and seeded into 24-well cluster plates (4 plates per flask) and used as follows:

Farnesyl Protein Transferase (FPT) Inhibition: FPT-1 Inhibitor Effect on Fe-Mediated Injury: Four 24-well cluster plates were seeded with HK-2 cells and each plate was divided into six treatment groups as follows: 1) control incubation; 2) incubation with 10 μmol/L of FPT-1 inhibitor (dissolved in distilled water, cat. no. 344153; Calbiochem, San Diego, CA); 3) incubation with 25 μmol/L of FPT-1 inhibitor; 4) incubation with 7.5 μmol/L of FeHQ; 5) addition of 10 μmol/L of FPT-1 inhibitor, followed 6 hours later by the addition of the above Fe challenge; and 6) addition of 25 μmol/L of FPT-1 inhibitor, followed 6 hours later by the Fe challenge. Eighteen hours after the addition of the Fe challenge, cell injury was assessed by percentage of lactate dehydrogenase (LDH) release.[1]

FPT-1 Inhibitor Effect on ADC-Mediated Injury: Four plates of HK-2 cells were established plus or minus the FPT-1 inhibitor doses noted above. After a 6-hour pretreatment period, the cells in each plate were subjected to either the ADC challenge or to incubation with ADC vehicle. Cell injury was assessed 18 hours later by percentage of LDH release.

Impact of FPT-II Inhibitor on Fe and ATP Depletion Mediated Cell Injury: To further determine the impact of farnesyl protein transferase inhibition on cell injury responses, a second inhibitor was tested: farnesyl protein transferase II inhibitor (FPTI-II) (in distilled water, catalog no. 344152; Calbiochem). In brief, the above described FeHQ and ADC challenge experiments were repeated four times as noted above, but substituting a single dose (25 μmol/L) of FPTI-II and/or the ADC and/or the FeHQ challenge. Eighteen hours after challenge, percentage of LDH release was assessed.

Geranylgeranyl Transferase (GGT) Inhibition: Impact on Fe-Mediated Injury. HK-2 cells were cultured in four 24-well plates as follows: 1) control incubation; 2) incubation with 0.5 μmol/L of a geranylgeranyl transferase inhibitor (GGTI) (catalog no. 345883; Calbiochem); 3) incubation with 1.0 μmol/L of GGTI; 4) incubation with 7.5 FeHQ; 5) incubation with 0.5 μmol/L GGTI, followed 6 hours later by the addition of FeHQ; and 6) incubation with 1.0 μmol/L GGTI, followed 6 hours later with FeHQ. Percentage of LDH release was assessed 18 hours after Fe addition.

Impact on ATP Depletion/Ca Overload Injury: The above experiment was repeated, but substituting the ADC for the FeHQ challenge.

Squalene Synthase Inhibition: Effects on Fe and ATP Depletion Induced Cell Injury

Zaragozic acid A (squalestatin-1) is a highly specific inhibitor of squalene synthase, the final regulated step of cholesterol biosynthesis.[34] Hence, inhibition at this stage permits more direct assessment of the impact of decreased cholesterol production than does statin-mediated upstream blockade of the entire mevalonate pathway.[22,23] Zaragozic acid A (ZGA) was kindly provided by Leslie Koch, Scientific Liaison, Merck Pharmaceuticals, West Point, PA. Four 24-well plates of HK-2 cells were each divided into six treatment groups: 1) control incubation; 2) addition of 5 μmol/L of ZGA (in distilled water); 3) addition of 10 μmol/L of ZGA; 4) addition of either the FeHQ or the ADC challenge; 5) 5 μmol/L of ZGA and either the FeHQ or ADC challenge; and 6) 10 μmol/L of ZGA and either the FeHQ or the ADC challenge (these challenges were added 6 hours after ZGA addition). Cell injury was assessed 18 hours later by percentage of LDH release. (Note: It had previously been confirmed that ZGA in the doses used decreases cholesterol synthesis in HK-2 cells.)

HMGCR mRNA Analysis by Reverse Transcriptase (RT)-PCR

RT-PCR was used to measure HMGCR and GAPDH mRNA in total RNA isolated from mouse renal cortex and HK-2 cells. Renal cortical or HK-2 cell samples, obtained as discussed above, were immediately placed into Trizol reagent (Invitrogen Life Technologies, Carlsbad, CA). Using the manufacturer's instructions, total RNA was extracted. The final RNA pellet was brought up in RNase-free water to an approximate concentration of 3 mg/ml. The samples were electrophoresed for 30 minutes through 1.2% agarose containing ethidium bromide (Sigma Chemical Co.) to ensure lack of degradation of the samples (preservation of 18S and 28S ribosomal RNA).

Table 1. Primer Sequences for RT-PCR Analysis of HMGCR

Genes	Primer sequence	PCR product size
HMGCR	5′-GGGACGGTGACACTTACCATCTGTATGATG-3′ 5′-ATCATCTTGGAGAGATAAAACTGCCA-3′	882 bp
GAPDH	5′-CTGCCATTTGCAGTGGCAAAGTGG-3′ 5′-TTGTCATGGATGACCTTGGCCAGG-3′	439 bp

Primer sequence used for the analysis of HMGCR. GAPDH served as the housekeeping gene.

Reverse transcription was performed using the First-Strand Synthesis Kit for RT-PCR (Ambion Inc., Austin, TX). The RT reaction was performed in a RNase-free tubes by first adding ~1 μg of RNA to a volume of diethyl pyrocarbonate-treated water (giving a total volume of 10 μl). After adding 2.0 μl of oligo-dt primer and 4 μl of dNTP mix (0.25 mmol/L each), the reaction was incubated at 72°C for exactly 3 minutes, and then rapidly quenched on ice. RT components included 2 μl of 10× buffer (final composition of 50 mmol/L Tris-HCl, pH 8.3, 75 mmol/L KCl, 3 mmol/L $MgCl_2$, 1 μl of recombinant RNase inhibitor (10 U/μL), and 1 μl of M-MLV reverse transcriptase (100 U/μg RNA), added as per the manufacturer's instructions. The total reaction volume of 20 μl was mixed and incubated at 42°C for 1 hour. The reaction was stopped by heating at 94°C for 10 minutes and immediately stored on ice until PCR.

The PCR was performed using the First-Strand Synthesis Kit for RT-PCR (Ambion Inc.), with HMGCR- and GAPDH-specific primers for mice (Integrated DNA Technologies, Coralville, IA). The specific primers were designed with 50 to 60% GC composition (Table 1). The resultant calculated high melting temperature (T_m) (>75°C) allows for a stringent annealing temperature in the PCR cycles. After RT, 47 μl of a PCR master mix, containing all PCR components and primers, was added to tubes containing 3 μl of cDNA. For the individual HMGCR and GAPDH reactions, 10 to 50 pmol of sense and anti-sense primers were used. In the hybrid reaction, in which HMGCR and GAPDH are assayed together, 50 pmol of each sense and anti-sense primer was used. Deoxynucleotides were added to a final concentration of 0.125 mmol/L for each reaction. Reaction buffer (10×) was diluted (1:10) to a final composition of: 10 mmol/L Tris-HCl, pH 8.3, 50 mmol/L KCl, and 1.5 mmol/L $MgCl_2$. After the samples were overlaid with mineral oil, the tubes are placed in a DNA thermal cycler. The thermal cycler was programmed as follows: first, incubation at 94°C, 5 minutes (initial melt); second, 25 cycles of the following sequential steps: 94°C, 1 minute (melt); 57°C, 1 minute (anneal); 72°C, 1 minute (extend). The last incubation was at 72°C for 7 minutes (final extension). PCR product analysis was conducted with 2% agarose gel electrophoresis and ethidium bromide staining. cDNA bands were visualized and quantified by densitometry using a Typhoon 8600 scanner (Amersham Pharmacia Biotech, Piscataway, NJ). HMGCR cDNA bands were expressed as a ratio to the simultaneously obtained GADPH cDNA bands, the latter used as a housekeeping gene. The HMGCR and GADPH PCR products were confirmed by DNA sequence analysis on 10% of the samples performed by automated cycle sequencing using ABI 373 DNA sequencer (Perkin Elmer). HK-2 cell samples were analyzed in an analogous manner to that described above.

Methods for Western Blot Analysis

Protein extracts were prepared from mouse cortical tissue samples and from HK-2 cells and subjected to Western blotting using general methodologies previously described from this laboratory.[5,6] The following reagents were used for each of the test proteins: 1) SREBP-1: primary antibody: mouse anti-SREBP-1 monoclonal antibody (catalog no. 67651A; PharMingen, San Diego, CA); secondary antibody: sheep anti-mouse IgG peroxidase-linked, species-specific, whole antibody (catalog no. NA931; Amersham Pharmacia, Piscataway, NJ); SREBP-2: primary antibody: mouse anti-SREBP-2 monoclonal antibody (catalog no. 67361A, Pharmingen); secondary antibody, as noted above; 3) Rho: Primary antibody: mouse IgG1 anti Rho; (catalog no. 610991; Transduction Laboratories, San Diego, CA); secondary antibody, as above; 4) Ras primary antibody: mouse pan Ras (catalog no. OP22; Oncogene Research Products, Boston, MA); secondary antibody, as above. NuPage 12% gels (Vitrogen, San Diego, CA) were used for Ras and Rho electrophoresis. Ten percent sodium dodecyl sulfate-polyacrylamide gel electrophoresis gels (BioRad, Hercules, CA) were used for SREBP-1 and -2 electrophoresis. Antibody dilutions were as per the manufacturer's instructions. Protein detection was by enhanced chemiluminescence.[5,6]

Calculations and Statistics

All values are presented as means ± 1 SEM. Statistical comparisons were performed by either paired or unpaired Student's *t*-test. If multiple comparisons were made, the Bonferroni correction was applied.

Results

HMGCR mRNA Analysis

Renal Cortical HMGCR mRNA after in Vivo *Ischemic Injury*

As shown in Figure 1, renal cortical HMGCR mRNA was suppressed by ~25% and 65% after 10 minutes of ischemia and either 1 hour or 24 hours of reflow, respectively. Twenty-four hours after the 30-minute ischemic insult, an ~60% decrease in HMGCR mRNA was ob-

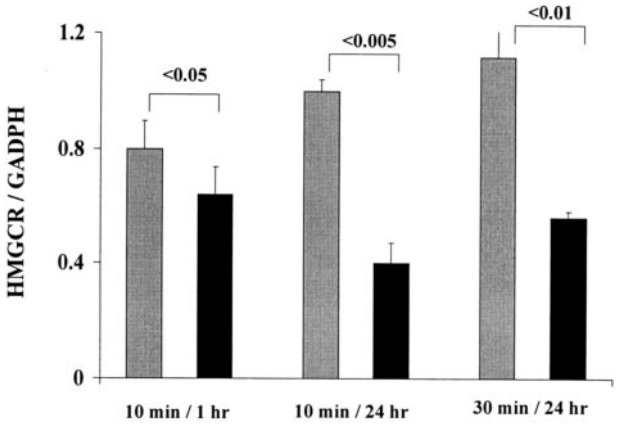

Figure 1. . HMGCR mRNA after *in vivo* ischemic-reperfusion injury. HMGCR mRNA values (factored by GADPH) were significantly depressed after 10 minutes of ischemia and either 1 hour or 24 hours of reflow. Similarly, a more severe ischemic insult (30 minutes) followed by 24 hours of reflow induced an ~60% reduction in renal-cortical HMGCR mRNA.

served. The BUN for the latter animals was 140 ± 25 mg/dL (*versus* controls 22 ± 2 mg/dL, $P < 0.01$).

Renal Cortical mRNA Expression after Glycerol-Mediated Injury

Renal cortical HMGCR mRNA was not significantly altered at 2 hours after glycerol injection (Figure 2). However, by 4 hours, an ~25% increase was apparent (Figure 2, left). The HMGCR mRNA elevation persisted 24 hours after glycerol injection, a time corresponding with renal cortical cholesterol overload.[1,4] The corresponding 24-hours BUNs for the after glycerol and control mice were 168 ± 19 and 26 ± 1 mg/dL, respectively ($P <$ 0.0001, unpaired *t*-test).

Renal Cortical and Hepatic mRNA after Fe (Venofer)-Induced Injury

As shown in Figure 3, hepatic HMGCR mRNA values were ~3.5 times higher in liver *versus* kidney ($P <$ 0.0002), consistent with the fact that the liver is the dominant site of cholesterol synthesis. Injection of Fe Venofer caused ~50% and 30% reductions in hepatic and renal cortical HMGCR mRNA values, respectively. Thus, this form of injury recapitulated the HMGCR mRNA changes observed after ischemic, rather than glycerol, injury.

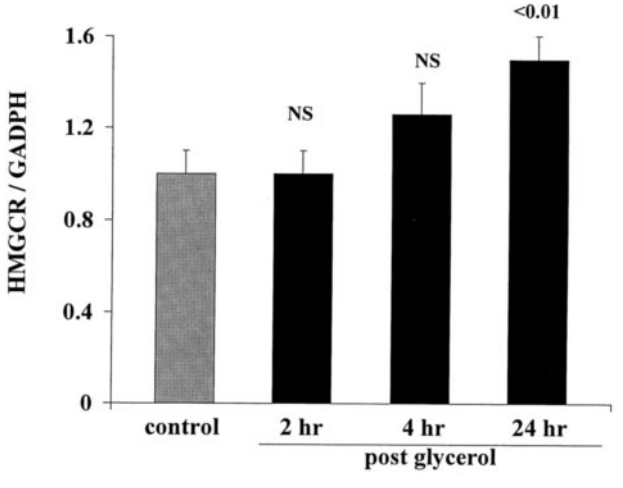

Figure 2. HMGCR mRNA levels after glycerol-mediated *in vivo* renal injury. HMGCR mRNA values did not differ from controls at 2 hours after glycerol injection. However, at both 4 and 24 hours after glycerol injection, modest, increases were apparent.

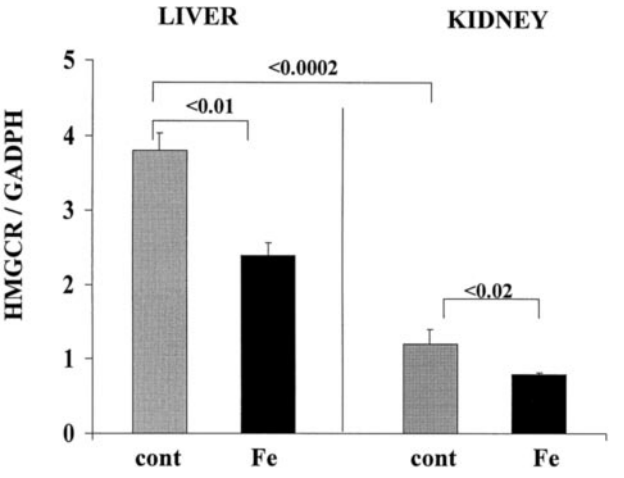

Figure 3. HMGCR mRNA values in liver and renal cortical extracts 3 hours after Fe Venofer injection. HMGCR mRNA values in both liver (**left**) and kidney (**right**) were significantly lowered after the Fe Venofer injection. Note the significantly higher values in control liver *versus* control (cont) kidney samples (consistent with the liver being the dominant site of cholesterol synthesis).

Hepatic HMGCR mRNA after Statin Therapy

The validity of the HMGCR mRNA analysis was confirmed by the observation that statin therapy caused hepatic HMGCR mRNA values to rise to 9.0 ± 0.07 from control values of 3.6 ± 0.05 ($P < 0.005$).

HK-2 Cell HMGCR mRNA after Fe and ATP Depletion/Ca Ionophore Injury

After a 4-hour FeHQ challenge, a time preceding lethal cell injury, HK-2 cell HMGCR mRNA levels were slightly suppressed, as depicted at the left of Figure 4. By 24 hours after Fe-induced injury, much more profound HMGCR mRNA reductions were apparent, with values falling by ~65%, compared to controls (Figure 4, middle). Four hours of ADC injury also caused significant reductions in HK-2 cell HMGCR mRNA content (Figure 4, right).

SREBP-1 Expression in HK-2 Cells in Response to Injury

Fe-Mediated Injury

As shown on the top half of Figure 5, three distinct bands were seen by Western blotting of HK-2 cells using anti-SREBP-1 antibody. One major and one minor band were seen at ~120 and 115 kd, respectively (consistent with uncleaved SREBPs-1a/c). A modest band at ~70 kd was also observed, consistent with active SREBP-1. No change in this profile was observed after 1 hour of Fe

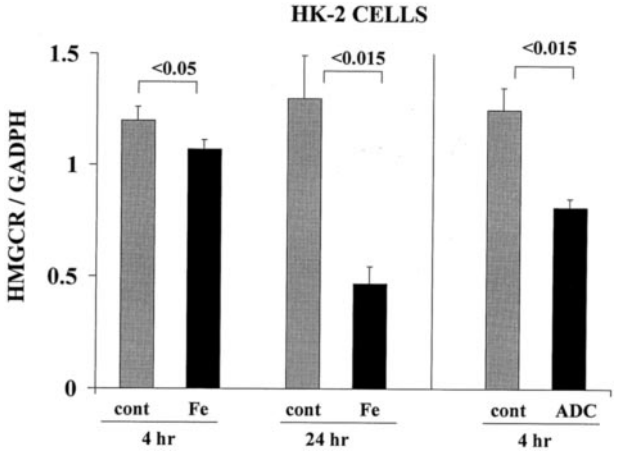

Figure 4. HMGCR mRNA in HK-2 cells after FeHQ- or ATP depletion/Ca ionophore-induced injury. Falling HMGCR mRNA values were observed from 4 hours to 24 hours after FeHQ exposure, compared to control incubated cells. Four hours of ADC also lowered HMGCR mRNA.

mediated injury (not shown). However, by 4 hours after Fe injury, marked decreases in both the 120- and 70-kd bands were apparent.

ATP Depletion Injury

SREBP-1 responses to the ADC challenge are depicted in the bottom half of Figure 5. As with the Fe challenge, no changes were observed after 1 hour of injury (not shown). However, by 4 hours of injury, changes similar to those observed with Fe treatment were observed: a marked decrease in both the dominant inactive (~120 kd) and active (~70 kd) bands. A slight increase in the 115-kd inactive band was apparent.

SREBP-2 Expression after HK-2 Cell Injury

Fe-Mediated Injury

As shown at the top of Figure 6, five bands were apparent in the control cells: two high molecular weight

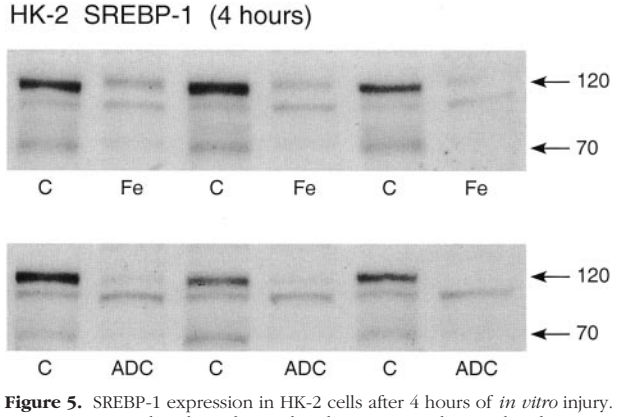

Figure 5. SREBP-1 expression in HK-2 cells after 4 hours of *in vitro* injury. SREBP-1 appeared as three distinct bands: a major and minor band at ~120 and ~115 kd, and another moderate band at ~70 kd. After 4 hours of FeHQ (Fe)-mediated injury (**top**), there were clear decreases in the 120-kd (inactive) and 70-kd (active) bands. Four hours of ADC injury (**bottom**) also caused a similar pattern. C, control incubations.

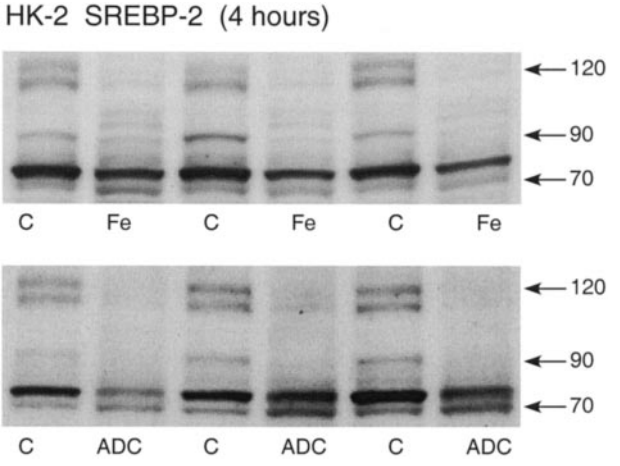

Figure 6. SREBP-2 expression in HK-2 cells after 4 hours of *in vitro* injury. SREPB-2 injury. Five bands were apparent in the control cells: two high molecular weight (~120 kd), two low molecular weight bands (~70 kd), and one band at ~90 kd. After 4 hours of Fe treatment, marked decreases in the ~120-kd and ~90-kd bands were observed (**top**). However, no consistent reciprocal increases in the active ~70-kd bands were apparent. ADC treatment (**bottom**) essentially reproduced the results achieved by FeHQ: there were clear decreases in the 120- and 90-kd inactive SREBP-2 bands without a reciprocal increase in lower molecular weight active bands. C, control incubations.

(~120 kd), two low molecular weight bands (~70 kd), and one band at ~90 kd. No changes were observed after 1 hour of Fe treatment (not shown). After 4 hours of Fe treatment, there were marked decreases in the ~120-kd and ~90-kd bands. However, no consistent reciprocal increases in the active ~70-kd bands were apparent.

ATP Depletion Injury

As shown in the bottom of Figure 6, ADC treatment essentially reproduced the results achieved by FeHQ: there was a clear decrease of 120- and 90-kd inactive SREBP-2 bands with no reciprocal increase in the low molecular weight active bands.

Twenty-Four-Hour Fe and Mevastatin Treatment

To test whether the 70-kd band reflected active SREBP-2, HK-2 cells were probed after 24 hours of mevastatin (M) treatment (which should up-regulate active SREBP-2).[18,19] As shown at the top of Figure 7, mevastatin did, indeed, increase active (70 kd) SREBP-2, consistent with HMGCR enzyme inhibition with a secondary increase in its relevant transcription factor. In contrast, Fe therapy essentially obliterated one of the two active SREBP-2 bands.

Unlike the changes observed in SREBP-2, statin treatment did not alter active SREBP-1 (Figure 7, bottom). This lack of response with statin therapy is consistent with the predilection of SREBP-2, rather than SREBP-1, to control cholesterol homeostasis.[20,21] Fe therapy for 24 hours also did not increase active SREBP-1.

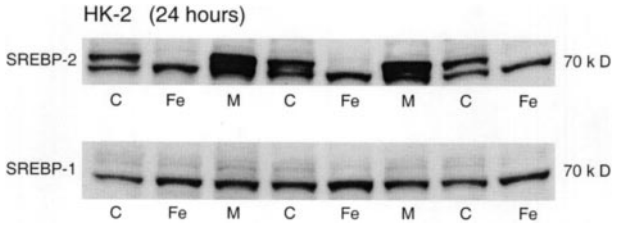

Figure 7. SREBP-1 and -2 after 24 hours of mevastatin or Fe treatment. HK-2 cells were incubated with either mevastatin (M) or FeHQ (Fe) for 24 hours, followed by assessment of SREBP-1 and -2 active (70 kd) bands. As can be seen, M caused a dramatic up-regulation of active SREBP-2. Conversely, Fe had the opposite effect, eliminating one of the two bands. Neither M nor Fe impacted the SREBP-1 active band (the former consistent with statin's preferential effect on SREBP-2; as per text). C, control incubations.

Assessments of Ras and Rho Prenylation

Renal Cortical Rho Expression

Rho was apparent as two distinct, but closely related, bands at ~29 kd (Figure 8). The upper and lower bands corresponded to unprenylated and prenylated moieties, respectively (based on the nonprenylated Rho standard, "Std," presented in the far left lanes). No apparent differences in distribution between the unprenylated *versus* the prenylated bands were apparent 24 hours after glycerol (G) or ischemic (I) injury compared to the controls (C) (Figure 1, rows 1 and 2, respectively). To gain confirmation of this issue, each of the bands was scanned and density ratios (prenylated divided by unprenylated band) were calculated for each sample. The values were as follows: control tissues, 0.73 ± 0.05; ischemia (I), 0.71 ± 0.01; and after glycerol (G), 0.70 ± 0.05 (all NS). The corresponding BUNs for these experiments were postischemic ARF, 189 ± 14 mg/dL; controls, 26 ± 2 mg/dL ($P < 0.001$); after glycerol ARF, 167 ± 38 mg/dL; controls, 27 ± 3 mg/dL ($P < 0.01$).

HK-2 Cell Rho Expression

As shown in the third row of Figure 8, the FeHQ challenge did not alter Rho prenylation, either by visual inspection or after quantitation of the prenylated *versus* nonprenylated bands (ratios: Fe, 0.59 ± 0.02; controls, 0.6 ± 0.01; NS). As expected, mevastatin (M) treatment noticeably decreased the prenylated band, a result that, when quantified, achieved statistical significance (mevastatin 0.45 ± 0.01 *versus* control 0.6 ± 0.01; $P < 0.02$) thus serving as a positive control.

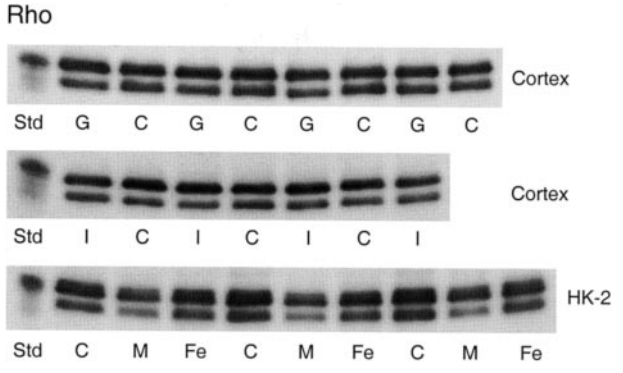

Figure 8. Rho expression 24 hours after glycerol- or ischemia-mediated *in vivo* injury or 24 hours after Fe or mevastatin treatment of cultured HK-2 cells. Prenylated Rho appears as the lower band (~21 kd) whereas the upper band corresponds to the unprenylated moiety (see standard; Std). No obvious change in the relative or absolute expression of either Rho form is apparent after the glycerol (G) or ischemic (I) challenges, compared to sham-treated controls (C) (**top** and **middle rows**, respectively). Mevastatin (M) caused an obvious decrease in prenylated Rho in HK-2 cells (**bottom row**). Conversely FeHQ-mediated injury had no impact absolute or relative HK-2 cell Rho expression.

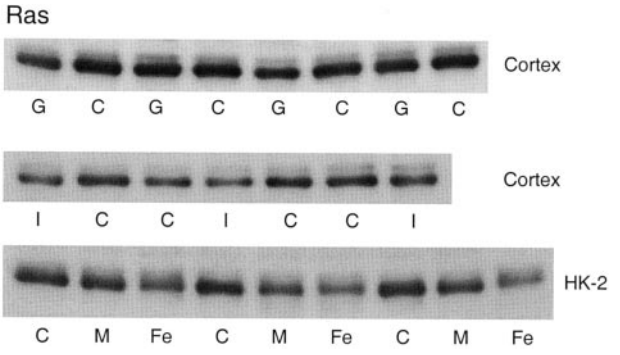

Figure 9. Ras expression 24 hours after glycerol- or ischemia-mediated *in vivo* injury or 24 hours after Fe or mevastatin treatment of cultured HK-2 cells. Ras appears as two closely associated bands that were not completely separated: the **top faint band** and the **bottom band** represent the unprenylated and prenylated forms, respectively. Neither glycerol- or ischemia-induced renal failure altered the pattern of Ras expression in renal cortical extracts. Fe, and to a lesser extent, mevastatin (M), appeared to induce mild decrements in the prenylated band. Thus, in sum, these results suggest that renal tubular injury does not evoke an increase in Ras prenylation.

Renal Cortical Ras Expression

Ras appeared as one minor (Figure 9, top) and one major (Figure 9, bottom) closely associated pancaked bands at ~21 kd, which could not be separately analyzed by densitometry (Figure 9). However, by visual inspection, the bottom, prenylated form, did not appear to increase in response to either the glycerol (G) or the ischemic (I) challenge (consistent with the findings of the Rho analysis, indicating unaltered prenylation after injury despite previously documented cholesterol accumulation).

HK-2 Cell Ras Expression

As shown in the third row of Figure 9, 18 hours after FeHQ-induced HK-2 injury, no apparent increase in Ras prenylation was observed. Rather, a Fe-induced tendency toward diminished, rather than increased, prenylation existed. Mevastatin (M) appeared to only slightly decrease Ras prenylation, compared to its more dramatic effect on the prenylation of Rho (Figure 9, line 3).

HK-2 Cell Injury: Farnesyl- and Geranylgeranyl-Protein Transferase Inhibition

FPTI-1

As shown in the left hand panel of Figure 10, treatment of HK-2 cells with 5 μmol/L of FPT-1 inhibitor (FPTI-1) caused no HK-2 cell death. However, 10 μmol/L of FPTI-1 did cause a very slight, but significant (2%; $P < 0.01$) increase in LDH release (indicating bioactivity of the in-

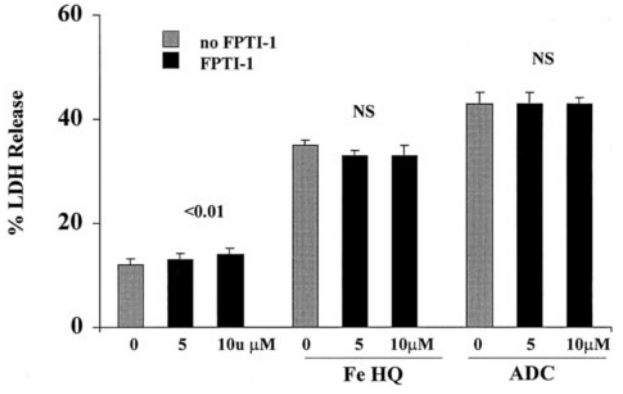

Figure 10. Effect of farnesyl protein transferase inhibitor-1 (FPTI-1) on the severity of FeHQ and ADC injury. HK-2 cells were incubated for 6 hours with FPTI-1 (0, 5, or 10 μmol/L concentrations). They were then either left under these conditions for an additional 18 hours, or they were exposed to either the oxidant (FeHQ) or ADC. Cell injury was assessed by percentage of LDH release 18 hours later. FPTI-1 induced slight toxicity in the absence of the Fe or ADC challenge ($P < 0.01$). However, FPTI-1 treatment did not significantly alter the extent of either Fe- or ADC-mediated cell death.

hibitor). However, neither FPTI-1 dose significantly worsened the severity of FeHQ- or ATP depletion (ADC)-mediated cell death.

FPTI-2

Incubation with 25 μmol/L of FPTI-2 inhibitor (FPTI-2) caused more overt cytotoxicity than did 10 μmol/L of FPTI-1 (10% increase in percent of LDH release over controls; Figure 11, left). When added to cells undergoing the FeHQ challenge, a modest increase in LDH release was observed. However, this simply seemed to be because of FPTI-2's independent cytotoxic effect (ie, there was no potentiation of Fe-induced injury). Further suggesting that FPTI-2 was not sensitizing cells to injury was the observation that it slightly lessened, rather than increased, ADC-mediated cell death (Figure 11, right; $P < 0.02$).

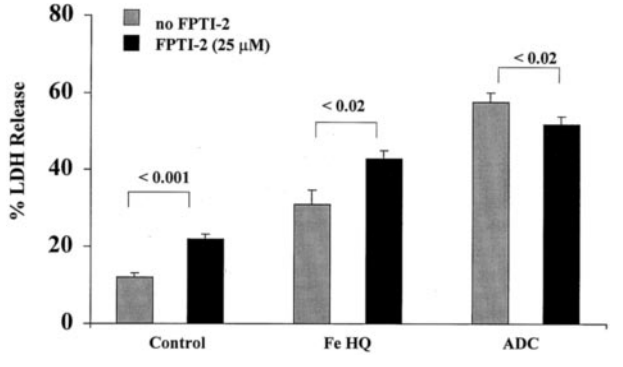

Figure 11. Effect of farnesyl protein transferase inhibitor 1 (FPTI-2) on the severity of FeHQ or ADC injury. These experiments were conducted exactly as described above for the FPTI-1 experiments, with the exception that they were conducted with a single dose of a second farnesyl protein transferase inhibitor (FPTI-2). This inhibitor exerted a mild direct cytotoxic effect under control incubation conditions. This same degree of toxicity was apparent in the Fe-exposed cells (ie, the FPTI-2-induced increase in Fe-associated LDH release was the same as it was in control cells, indicating no potentiation of Fe-induced injury). In contrast, FPTI-2 slightly decreased cell death in the ADC-challenged cells. In sum, these data indicate that FPTI-2 did not predispose to Fe- or ATP/Ca ionophore-mediated tubular cell death.

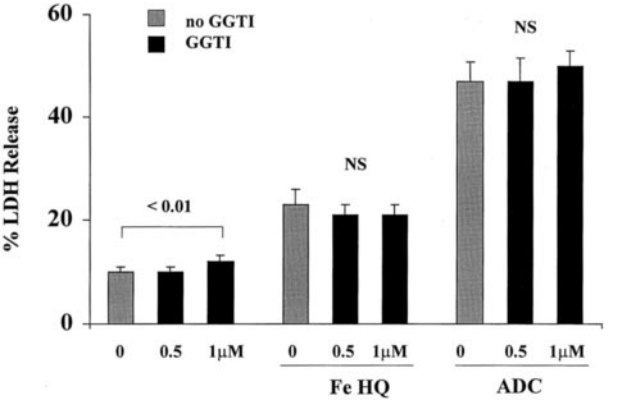

Figure 12. Effect of geranylgeranyl protein transferase inhibitor (GGTI) on the severity of FeHQ or ADC injury. These experiments were conducted in a manner analogous to those presented in Figure 10. The inhibitor induced mild dose-dependent cytotoxicity under control conditions (indicating bioactivity). However, it did not significantly impact either FeHQ- or ATP depletion/Ca ionophore (ADC)-induced tubular cell injury, as assessed by percentage of LDH release.

GGTI

As shown in Figure 12, left, the geranylgeranyl protein transferase inhibitor (GGTI) caused a very slight, but significant, increase in percentage of LDH release at the 1 μmol/L concentration ($P < 0.01$), confirming its bioactivity. However, neither inhibitor dose significantly altered the severity of FeHQ- or ADC-mediated cell death.

HK-2 Cell Injury: Impact of Zaragozic Acid Treatment

As demonstrated in Figure 13, squalene synthase inhibition with zaragozic acid (ZGA) had a minimal impact on HK-2 cell viability in the absence of either the iron or ATP depletion challenge. In the presence of either Fe or ATP depletion (ADC) injury, ZGA caused a substantial, dose-dependent, and significant increase in tubular cell death. This was particularly true with the ADC injury model in which 10 μmol/L of ZGA increased the percentage of LDH release from 37 to 67%.

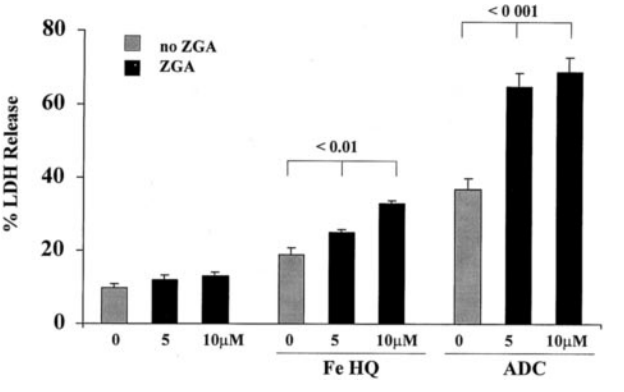

Figure 13. The effect of zaragozic acid A (ZGA) on the severity of FeHQ-mediated oxidant stress or ADC injury. ZGA had virtually no effect on HK-2 cell viability under control incubation conditions. However, it induced dose-dependent increases in both Fe- and ADC-induced lethal cell injury, as assessed by percentage of LDH release.

Discussion

In our previous studies of stress-mediated renal cholesterol accumulation, increases in renal cortical HMGCR protein were observed after glycerol- (heme Fe), and ischemia-induced ARF.[5] Fe-induced injury, imposed on cultured HK-2 cells, also caused dose-dependent HMGCR protein increments.[5] The latter supported our assumption that the observed renal cortical HMGCR enzyme increments reflected, at least in part, proximal tubular cell events. Given these past observations, the present study was undertaken, in part, to ascertain whether cell injury activates HMGCR transcription/translation, culminating in increased HMGCR protein, and ultimately cholesterol, content.

Tissue HMGCR enzyme levels reflect a multifaceted, regulated balance between enzyme production *versus* destruction via the ubiquitin-proteasomal pathway.[31] If transcriptional events are responsible for injury-evoked HMGCR enzyme increases, then a correlate of this process should be an increase in HMGCR mRNA. Conversely, if decreased catabolism causes enzyme accumulation, reduced HMGCR mRNA levels would be expected (ie, because of normal feedback suppression of its synthesis). The available *in vitro* data favor the latter possibility because at 4 hours after FeHQ- or ADC-induced HK-2 cell injury, falling, rather than rising, HMGCR message levels were observed; and also at 24 hours after FeHQ-induced HK-2 cell injury, a time of increased cholesterol and HMGCR enzyme expression, HMGCR mRNA was reduced by ~67%. To ascertain whether these *in vitro* results had an *in vivo* correlate, HMGCR message was also assessed after *in vivo* renal damage. In the case of ischemia/reperfusion, time-dependent decrements in renal HMGCR mRNA levels were observed. Venofer Fe, used to simulate *in vitro* FeHQ injury, also evoked significant renal (as well as hepatic) HMGCR mRNA reductions. When viewed together, these *in vitro* and *in vivo* data strongly suggest that although acute cellular stress can increase both HMGCR enzyme and cholesterol levels, these changes can also be dissociated from increases in HMGCR mRNA content. This is, at least, consistent with the notion that posttranscriptional/translational events, such as decreased ubiquitin-proteosomal catabolism, could cause HMGCR enzyme accumulation in postrenal injury states. One intriguing potential mediator for such a change could be injury-evoked heat shock protein induction. Because HMGCR enzyme and heat shock protein-70 levels closely correlate after renal injury,[5] it is intriguing to speculate that heat shock proteins might chaperone HMGCR enzyme, thereby stabilizing it, decreasing its degradation.[35] In this regard, it is also noteworthy that inhibition of the ubuiquitin-proteasomal pathway has been associated with cellular resistance to injury.[36,37] Whether such a result might be, in part, explained by an increase in HMGCR remains an intriguing question.

Given the complexity of HMGCR enzyme regulation, it should not simply be assumed that a single mechanism is responsible for its accumulation after all forms of cellular stress. Rather, differing types of injury might differentially impact the mechanisms that ultimately control HMGCR and cholesterol levels. Indeed, the current glycerol-induced ARF experiments underscore this concept. In striking contrast to all other test models of proximal tubular injury, glycerol-induced rhabdomyolysis was the only one to cause renal cortical HMGCR mRNA increments, reaching ~50% elevations by 24 hours after renal damage. As previously noted, glycerol-induced ARF is not simply a model of heme iron toxicity. Rather, multisystem organ dysfunction (muscle, heart, liver) with systemic cytokine release are all pathogenetically involved.[30] Whether these differences explain the rising HMGCR mRNA levels in this particular ARF model remains unknown. However, one point is clear: glycerol (rhabdomyolysis) and ischemic ARF each induce comparable cholesterol and HMGCR enzyme elevations[5] irrespective of whether HMGCR mRNA levels are elevated or depressed. This again suggests that HMGCR enzyme and cholesterol accumulation after cell injury predominantly reflect posttranscriptional events.

HMGCR mRNA expression is predominately regulated by SREBP transcription factors (SREBP-1b,c; SREBP-2) that reside in uncleaved (~115 to 125 kd), inactive, forms within the endoplasmic reticulum.[18–20] Under conditions of cellular cholesterol depletion, the SREBPs migrate from the endoplasmic reticulum to the Golgi apparatus, a process that is regulated by the cholesterol-sensing protein, SCAP (steroid cleavage activity protein).[18–20] Once within the Golgi, SREBPs undergo sequential cleavage by two distinct proteases (S1P, S2P). In pathological states, this process can also be effected by caspase-3.[38] After cleavage, the activated SREBPs (~60 to 80 kd) migrate to the nucleus where they bind to steroid-responsive elements that regulate multiple genes that impact cholesterol/lipid biosynthesis and lipid endocytic processes (eg, low-density lipoprotein receptor density).[15,18–23] Although some functional overlaps in activities exist, SREBP-1 and SREBP-2 are thought to preferentially regulate fatty acid and cholesterol homeostasis, respectively.[39]

Given the observations that acute cell injury tends to lower HMGCR mRNA, one possible explanation could be direct RNA damage. This would then be expected to secondarily activate the SREBPs. Alternatively, if cell injury causes proteolytic SREBP disruption, a secondary decrease in HMGCR mRNA should result. To discriminate between these two possibilities, SREBP-1 and SREBP-2 were probed in HK-2 cells at 1, 4, and 24 hours after Fe and ATP depletion-mediated HK-2 cell injury. (Unfortunately, mouse tissues could not be probed because of lack of suitable antibodies.) By 4 hours after Fe or ATP depletion-induced HK-2 cell injury, clear decrements in high molecular weight (inactive) SREBPs were observed, consistent with proteolytic activation; however, no reciprocal increases in low molecular weight active SREBP fragments were observed. After 24 hours of Fe-induced injury, decreases in both active and inactive SREBP moieties were apparent. Confirming the validity of the used Western blotting was the finding of a marked increment in activated SREBP-2 with 24 hours of statin therapy. Thus, these results indicate that acute cell injury

can rapidly destroy SREBPs, a result that could secondarily explain the observed decrements in HMGCR mRNA. The mechanisms by which cell injury depleted the SREBPs remain unknown. However, in data not presented, caspase 3 inhibitors did not prevent this process.

Irrespective of the exact mechanisms controlling SREBP, HMGCR mRNA, and HMGCR protein expression after cell injury, the final result is cholesterol accumulation that seems to contribute to the so-called cytoresistance state. The evidence to support this mechanistic link is as follows: 1) statin-induced cholesterol reductions increase cellular vulnerability to attack;[1] 2) normalizing cell cholesterol levels in cytoresistant proximal tubules by chemical extraction reverses the cytoresistant state;[1] and 3) enzymatic cholesterol modification with either cholesterol oxidase or cholesterol esterase either induces overt cell injury or sensitizes tubular cells to superimposed attack.[1,7] Despite these observations, it is conceivable that each of these previously used pharmacological interventions could have impacted more than just cholesterol levels. For example, statin therapy can decrease farnesyl and geranylgeranylpyrophosphate, as well as cholesterol, synthesis.[22–26] Chemical cholesterol extraction, or enzymatic cholesterol modification, could also impact upstream molecules within the mevalonate pathway, eg, by diverting them into terminal cholesterol synthesis. Finally, injury-induced activation of the mevalonate pathway might enhance protein prenylation in addition to cholesterol levels. Because increased protein prenylation can confer a survival advantage in diverse cell lines,[24–28] this change, in addition to cholesterol build up, could play a key mechanistic role in cell injury responses. Hence, additional experiments were conducted to help discern the role of protein prenylation *versus* cholesterol accumulation in the expression of the cytoresistant state.

The first additional piece of evidence to suggest that cholesterol, and not enhanced protein prenylation, is the prime determinant of cytoresistance comes from the present mevalonate pathway inhibitor experiments. Neither of two farnesyl protein transferase inhibitors sensitized HK-2 cells to Fe- or ATP-depletion-mediated attack. Additionally, geranylgeranyl protein transferase inhibition did not increase Fe- or ATP-depletion-mediated HK-2 cell death. In striking contrast to the results obtained with isoprenoid transferase inhibitors, specific blockade of terminal cholesterol synthesis via squalene synthase inhibition dramatically sensitized HK-2 cells to both Fe and ATP depletion-induced attack. In sum, then, these results, obtained with three mevalonate/cholesterol pathway inhibitors, provide strong additional support for our previously advanced concept: that postinjury-induced increases in HMGCR/mevalonate pathway activity likely confers cytoresistance via an increase in cellular cholesterol content. Further supporting this conclusion are our present observations that renal cortical cholesterol accumulation in the setting of rhabdomyolysis and ischemic ARF each developed in the absence of any obvious increase in protein (Ras/Rho) prenylation events. Comparable *in vitro* results after a FeHQ challenge support these *in vivo* data. Indeed, to our knowledge, these are the first studies to demonstrate that ischemic/ATP depletion and oxidant cell injury occur independently of discernible changes in protein prenylation status. However, it is important to stress that although a change in prenylation of these proteins did not result, this clearly does not exclude a change in their activities. For example, Ras-GTP binding/Rho activity can potentially be impacted by a plethora of cellular signaling and pathophysiological events, ushered in by mediators of acute cell injury (eg, oxidative stress, reperfusion injury.[40–43]

In conclusion, the present studies demonstrate for the first time that acute ATP depletion or Fe-induced oxidative injury causes SREBP disruption within proximal tubular cells, and that acute reductions in HMGCR mRNA result. Furthermore, acute ischemic or Fe-induced *in vivo* injury also suppresses renal cortical HMGCR mRNA. These findings support the concept that injury-induced activation of the mevalonate pathway likely arises from posttranscriptional events (eg, HMGCR enzyme stabilization). However, a single operative mechanism for all injury models is unlikely. This is underscored by the current observations that the glycerol model of rhabdomyolysis up-regulates, rather than suppresses, renal cortical HMGCR mRNA. Finally, postrenal injury-induced cholesterol accumulation can be dissociated from a concomitant increase in protein (Ras/Rho) prenylation. This observation, plus the fact that squalene synthase, but not prenylation, inhibitors augment HK-2 cell injury support the concept that cholesterol accumulation, per se, is the dominant mechanism by which mevalonate pathway contributes to the postrenal injury cytoresistant state.

References

1. Zager RA, Burkhart KM, Johnson A, Sacks B: Increased proximal tubular cholesterol content: implications for cell injury and the emergence of "acquired cytoresistance." Kidney Int 1999, 56:1788–1797
2. Zager RA, Kalhorn T: Changes in free and esterified cholesterol: hallmarks of acute tubular injury and acquired cytoresistance. Am J Pathol 2000, 157:1007–1016
3. Zager RA, Johnson A, Anderson K, Wright S: Cholesterol ester accumulation: an immediate consequence of acute ischemic renal injury. Kidney Int 2001, 59:1750–1761
4. Zager RA, Andoh T, Bennett WM: Renal cholesterol accumulation: a durable response following acute and subacute renal insults. Am J Pathol 2001, 159:743–752
5. Zager RA, Johnson AC: Renal cortical cholesterol accumulation: an integral component of the systemic stress response. Kidney Int 2001, 60:2229–2310
6. Zager RA, Johnson A, Hanson S, dela Rosa V: Altered cholesterol localization and caveolin expression during the evolution of acute renal failure. Kidney Int (in press)
7. Zager RA: Plasma membrane cholesterol: a critical determinant of cellular energetics and tubular resistance to attack. Kidney Int 2000, 58:193–205
8. Zager RA: P glycoprotein-mediated cholesterol cycling: a potentially important determinant of proximal tubular cell viability. Kidney Int 2001, 60:944–956
9. Honda N, Hishida A, Ikuma K, Yonemura K: Acquired resistance to acute renal failure. Kidney Int 1987, 31:1233–1238
10. Nath KA, Haggard JJ, Croatt AJ, Grande JP, Poss KD, Alam J: The indispensability of heme oxygenase-1 in protecting against acute heme protein-induced toxicity in vivo. Am J Pathol 2000, 156:1527–1535
11. Leung N, Croatt AJ, Haggard JJ, Grande JP, Nath KA: Acute cholestatic liver disease protects against glycerol-induced acute renal failure in the rat. Kidney Int 2001, 60:1047–1057

12. Nath KA, Balla G, Vercellotti GM, Balla J, Jacob HS, Levitt MD, Rosenberg ME: Induction of heme oxygenase is a rapid, protective response in rhabdomyolysis in the rat. J Clin Invest 1992, 90:267–270
13. Zager RA, Baltes LA: Progressive renal insufficiency induces increasing protection against ischemic acute renal failure. J Lab Clin Med 1984, 103:511–523
14. Zager RA, Baltes LA, Sharma HM, Jurkowitz MS: Responses of the ischemic acute renal failure kidney to additional ischemic events. Kidney Int 1984, 26:689–700
15. Goldstein JL, Brown MS: Regulation of the mevalonate pathway. Nature 1990, 343:425–430
16. Bjorkhem I, Lund E, Rudling M: Coordinate regulation of cholesterol, 7α hydroxylase, and HMG-CoA reductase in the liver. Subcellular Biochemistry, vol 28, Cholesterol: Its Functions and Metabolism in Biology and Medicine. Edited by R Bittman. New York, Plenum Press, 1997
17. Edwards PA, Tabor D, Kast HR, Venkateswaran A: Regulation of gene expression by SREBP and SCAP. Biochim Biophys Acta 2000, 1529: 103–113
18. Thewke D, Kramer M, Sinensky MS: Transcriptional homeostatic control of membrane lipid composition. Biochemical Biophys Res Commun 2000, 273:1–4
19. Shimano H: Sterol regulatory element-binding proteins (SREBPs): transcriptional regulators of lipid synthetic genes. Prog Lipid Res 2001, 40:439–452
20. Sakai J, Rawson RB: The sterol regulatory element-binding protein pathway: control of lipid homeostasis through regulated intracellular transport. Curr Opin Lipidol 2001, 12:261–266
21. Nohturfft A, DeBose-Boyd RA, Scheek S, Goldstein JL, Brown MS: Sterols regulate cycling of SREBP cleavage-activating protein (SCAP) between endoplasmic reticulum and Golgi. Proc Natl Acad Sci USA 1999, 96:11235–11240
22. Brown MS, Goldstein JL: A proteolytic pathway that controls the cholesterol content of membranes, cells, and blood. Proc Natl Acad Sci USA 1999, 96:11041–11048
23. Edwards PA, Ericsson J: Sterols and isoprenoids: signaling molecules derived from the cholesterol biosynthetic pathway. Annu Rev Biochem 1999, 68:157–185
24. Jackson SM, Ericsson J, Edwards PA: Signaling molecules derived from the cholesterol biosynthetic pathway. Subcellular Biochemistry, vol 28. Cholesterol: Its Functions and Metabolism in Biology and Medicine. Edited by R Bittman. New York, Plenum Press, 1997
25. Xia Z, Tan MM, Wong WW, Dimitroulakos J, Minden MD, Penn LZ: Blocking protein geranylgeranylation is essential for lovastatin-induced apoptosis of human acute myeloid leukemia cells. Leukemia 2001, 15:1398–1407
26. McGuire TF, Sebti SM: Geranylgeraniol potentiates lovastatin inhibition of oncogenic H-Ras processing and signaling while preventing cytotoxicity. Oncogene 1997, 14:305–312
27. Limura O, Vrtovsnik F, Terzi F, Friedlander G: HMG-CoA reductase inhibitors induce apoptosis in mouse proximal tubular cells in primary culture. Kidney Int 1997; 52: 962–972
28. Padayatty SJ, Marcelli M, Shao TC, Cunningham GR: Lovastatin-induced apoptosis in prostate stromal cells. J Clin Endocrinol Metab 1997, 82:1434–1439
29. Stark Jr WW, Blaskovich MA, Johnson BA, Qian Y, Vasudevan A, Pitt B, Hamilton AD, Sebto SM, Davies P: Inhibiting geranylgeranylation blocks growth and promotes apoptosis in pulmonary vascular smooth muscle cells. Am J Physiol 1998, 275:L55–L63
30. Zager RA: Heme protein induced tubular cytoresistance: expression at the plasma membrane level. Kidney Int 1995, 47:1336–1345
31. Zager RA: Rhabdomyolysis and myohemoglobinuric acute renal failure. Kidney Int 1996, 49:314–326
32. Zager RA, Johnson AC, Hanson SY, Wasse M: Parenteral iron formulations: a comparative toxicologic analysis and mechanism of cell injury. Am J Kidney Dis 2002, 40:90–103
33. Ryan MJ, Johnson G, Kirk J, Fuerstenberg SM, Zager RA, Torok-Storb B: HK-2: an immortalized proximal tubule epithelial cell line from normal human kidney. Kidney Int 1994, 45:48–57
34. Iwata M, Herrington JB, Zager RA: Protein synthesis inhibition induces cytoresistance in cultured proximal tubular (HK-2) cells. Am J Physiol 1995, 268:F1154–F1163
35. Petras SF, Lindsey S, Harwood Jr HJ: HMG-CoA reductase regulation: use of structurally diverse first half-reaction squalene synthetase inhibitors to characterize the site of mevalonate-derived nonsterol regulator production in cultured IM-9 cells. J Lipid Res 1999, 40:24–38
36. Ravid T, Doolman R, Avner R, Harats D, Roitelman J: The ubiquitin-proteasome pathway mediates the regulated degradation of mammalian 3-hydroxy-3-methylglutaryl-coenzyme A reductase. J Biol Chem 2000, 275:35840–35847
37. Bush KT, Goldberg AL, Nigam SK: Proteasome inhibition leads to a heat-shock response, induction of endoplasmic reticulum chaperones, and thermotolerance. J Biol Chem 1997, 272:9086–9092
38. Volloch V, Mosser DD, Massie B: Sherman MY: Reduced thermotolerance in aged cells results from a loss of an hsp72-mediated control of JNK signaling pathway. Cell Stress Chaperones 1998, 3:265–271
39. Utz PJ, Anderson P: Life and death decisions: regulation of apoptosis by proteolysis of signaling molecules. Cell Death Differ 2000, 7:589–602
40. Ou J, Tu H, Shan B, Luk A, DeBose-Boyd RA, Bashmakov Y, Goldstein JL, Brown MS: Unsaturated fatty acids inhibit transcription of the sterol regulatory element-binding protein-1c (SREBP-1c) gene by antagonizing ligand-dependent activation of the LXR. Proc Natl Acad Sci USA 2001, 98:6027–6032
41. Fantl WJ, Johnson DE, Williams LT: Signaling by receptor tyrosine kinases. Annu Rev Biochem 1993, 62:453–481
42. Deora AA, Win T, Vanhaesebroeck B, Lander HM: A redox triggered ras-effector interaction. Recruitment of phosphatidylinositil 3′-kinase to Ras by redox stress. J Biol Chem 1998, 273:29923–29928
43. Aikawa R, Komuro I, Yamazaki T, Zou Y, Kudoh S, Tanaka M, Shiojima I, Hiroi Y, Yazaki Y: Oxidative stress activates extracellular signal-regulated kinase through Src and Ras in cultured cells. J Clin Invest 1997, 100:1813–1821